Lawrence Berkeley National Laboratory

Title

Near-K-edge single, double, and triple photoionization of C+ ions

Permalink

Journal

ISSN

Authors

Müller, A
Borovik, A
Buhr, T
et al.

Publication Date

DOI

Near-K-edge single, double, and triple photoionization of C$^+$ ions

A. Müller,[1,*] A. Borovik, Jr.,[2] T. Buhr,[2] J. Hellhund,[1] K. Holste,[2] A. L. D. Kilcoyne,[3] S. Klumpp,[4] M. Martins,[5] S. Ricz,[6]
J. Viefhaus,[7,†] and S. Schippers[2]

[1]*Institut für Atom- und Molekülphysik, Justus-Liebig-Universität Gießen, 35392 Giessen, Germany*
[2]*I. Physikalisches Institut, Justus-Liebig-Universität Gießen, 35392 Giessen, Germany*
[3]*Advanced Light Source, Lawrence Berkeley National Laboratory, Berkeley, 94720-8225 California, USA*
[4]*DESY Photon Science, FS-FLASH-D, 22607 Hamburg, Germany*
[5]*Institut für Experimentalphysik, Universität Hamburg, 22761 Hamburg, Germany*
[6]*Institute for Nuclear Research, Hungarian Academy of Sciences, 4001 Debrecen, Hungary*
[7]*DESY Photon Science, FS-PE, 22607 Hamburg, Germany*

Single, double, and triple ionization of the C$^+$ ion by a single photon have been investigated in the energy range 286 to 326 eV around the K-shell single-ionization threshold at an unprecedented level of detail. At energy resolutions as low as 12 meV, corresponding to a resolving power of 24 000, natural linewidths of the most prominent resonances could be determined. From the measurement of absolute cross sections, oscillator strengths, Einstein coefficients, multielectron Auger decay rates, and other transition parameters of the main K-shell excitation and decay processes are derived. The cross sections are compared to results of previous theoretical calculations. Mixed levels of agreement are found despite the relatively simple atomic structure of the C$^+$ ion with only five electrons. This paper is a followup to a previous Letter [A. Müller *et al.*, Phys. Rev. Lett. **114**, 013002 (2015)].

I. INTRODUCTION

Carbon is the second most abundant heavy element (with atomic numbers $Z > 2$) in the universe next to oxygen. It is prominently present in all astrophysical environments. Moreover, it is the prime constituent of organic chemistry and the building block of life on Earth. In both collisionally ionized and photoionized gases, carbon atoms occur singly or multiply charged and the ions can serve as probes for the state of the plasma in which they are formed, be it of astrophysical or terrestrial origin. Important diagnostic techniques rely on the soft-x-ray spectroscopy of carbon ions, especially near the K edge [1].

Similar spectroscopic techniques based on the production and observation of the decay of K-vacancy states are employed to characterize the chemical environment of carbon atoms in molecules, clusters, and solids. When a K-shell electron is removed from a neutral carbon atom, the resulting ion is most likely in one of the C$^+$($1s2s^22p^2\ {}^2S,{}^2P,{}^2D$) states which then decay by emitting photons or electrons with characteristic energies. Identical terms can be excited from the ground state of C$^+$ ions by irradiation with photons of the same characteristic energies [2]. Resonance parameters and details of the transitions such as the natural widths, the oscillator strengths, and the exact wavelengths can be determined in photoionization experiments with C$^+$ ions.

An important aspect of K-shell excited C$^+$($1s2s^22p^2\ {}^2S,{}^2P,{}^2D$) states is their unique electronic configuration with four electrons in the L shell. Four electrons residing above a K-shell vacancy are the minimum required for observing triple-Auger decay in which one of the four electrons falls into the K vacancy while all three other electrons are ejected into the continuum in a correlated four-electron process. This process has been unambiguously identified in our preceding Letter [3].

Photoprocesses involving C$^+$ ions have been studied in previous experiments. Photoabsorption by boronlike C$^+$ ions was investigated by Jannitti *et al.* [4] with a technique using two laser-produced plasmas. Photoionization of C$^+$ ions has already been addressed in several merged-beam experiments. The valence-electron energy range has been studied by Kjeldsen *et al.* [5,6], while Schlachter *et al.* [2] explored the $1s \rightarrow 2p$ excitation resonances. In both cases, absolute single-ionization cross sections were determined. Theoretical calculations for K-shell photoabsorption by C$^+$ ions have produced cross sections using R-matrix techniques [1,2,7] and, indirectly, by the multiconfiguration Dirac-Fock method [8].

Measurements for the boronlike sequence of ions were recently extended to N^{2+} [9] and O^{3+} [10] by using the photon-ion merged-beam technique. Resonant K-shell excitation of boronlike Fe^{21+}($1s^22s^22p\ {}^2P_{1/2}$) was observed by detecting fluorescence photons and photoions [11,12] in experiments employing an electron beam ion trap. Deep-core photoexcitation of ions has recently been reviewed by Müller [13].

Because of the low density of ions in a beam, the presence of high detector backgrounds and limited photon flux available from synchrotron radiation sources, photoioniza-

*alfred.mueller@iamp.physik.uni-giessen.de
†Present address: Helmholtz-Zentrum Berlin, Department Optics and Beamlines, Berlin, Germany.

tion experiments involving K-vacancy production had been limited until recently to the strongest resonance features in the spectrum. Schlachter *et al.* [2] observed only $1s \rightarrow 2p$ transitions in C$^+$ at resolving powers 2400 to 5800. Gharaibeh *et al.* [9] measured the strongest $1s \rightarrow 2p$ and $1s \rightarrow 3p$ transitions in N^{2+} at resolving powers $E/\Delta E$ 4500 to 13 500. McLaughlin *et al.* [10] investigated the same transitions in O^{3+} at resolving powers $E/\Delta E$ 3200 to 5000. The ion-trap experiments involving K-vacancy production in B-like Fe^{21+} ions were restricted to the observation of an unresolved blend of Fe$^{21+}(1s2s^2 2p^2\ ^2P_{1/2})$ and Fe$^{21+}(1s2s^2 2p^2\ ^2D_{3/2})$ levels in the energy range 6583–6589 eV. The associated resonances were not directly measured on an absolute cross-section scale. The energy resolution in the particular measurement on Fe^{21+} was 1 eV corresponding to a resolving power of about 6600.

All those previous experiments were restricted to the single-ionization channel and a few isolated resonances. Since then, significant experimental progress has been achieved in that the energy ranges of experiments have been extended to the region beyond the K edge and multiple ionization up to the removal of three electrons from the initial ion was investigated for the lighter elements up to atomic number $Z = 10$ [3,14–17]. L-shell excitation and ionization in Fe$^+$ and M-shell vacancy production in singly and multiply charged xenon ions have been investigated by observing up to sixfold net ionization of the parent ion [18–20].

Here we report absolute cross-section measurements for photoionization of C$^+$ near the K edge. The experiments were performed at the photon-ion merged-beam setup PIPE (photon-ion spectrometer at PETRA III) [19] using monochromatized undulator radiation from the PETRA III synchrotron light source in Hamburg. Single and double ionization were investigated covering the whole range of $1s \rightarrow np$ ($n = 2,3,4,\ldots,\infty$) one-electron and $1s2s \rightarrow 2pn\ell$ ($n = 2,3,4,\ldots,\infty, \ell = 0,2$) two-electron excitations occurring well beyond the K-shell ionization threshold. For the strongest $1s \rightarrow 2p$ resonances and the immediate K-edge region, triple ionization was also observed. With the extended capabilities of the PIPE experiment, structures and processes in ionized atoms, molecules, and clusters can be observed which have not been previously accessible to experiments.

The present paper provides details of experiments and additional results from our previous work [3]. Emphasis in the previous publication was on the discovery and unambiguous demonstration of an elusive four-electron Auger process, the triple-Auger decay, in which three electrons are ejected in a single event while a fourth electron falls into a K-shell vacancy. The present paper focuses on the determination of absolute cross sections at very high-energy resolution and the information that can be derived from the combined results of absolute measurements of partial cross sections for different final channels and the natural widths of resonance lines.

This presentation is structured as follows. After this introduction, a brief overview of the experiment is provided with details specific to the present measurements. The experimental results are shown in detail. Photoabsorption cross sections for C$^+$ ions and decay parameters of core excited states are derived from the measurements and compared with the results of theoretical calculations as well as with measurements available

in the literature. After a summary and acknowledgments, an Appendix describes the formalism and procedure for the extraction of transition parameters from absolute photoionization cross sections.

II. EXPERIMENT

The experimental arrangement and procedures have been described in detail previously [17,19]. In short, C$^+$ ions were produced for the present measurements in an electron-cyclotron-resonance (ECR) ion source. The ions were accelerated to 6 keV and magnetically analyzed to obtain an isotopically pure beam, which was then transported to the interaction region, collimated, and merged with the photon beam available at beamline P04 [21] of PETRA III. The product ions were separated from the parent ion beam by a dipole magnet inside which the primary beam was collected in a large Faraday cup. The photoionized ions were passed through a spherical 180-deg out-of-plane deflector to suppress background from stray electrons, photons, and ions and then entered a single-particle detector with near-100% detection efficiency. The high brightness and flux of the photon beam (2×10^{11} s^{-1} at 288 eV energy and 12 meV bandwidth) permitted tight collimation of the ion beam (1.5 nA) and a significantly improved spatial overlap with the photon beam compared to earlier experiments. Form factors [17,19,22] in the cross-section measurements were between 3460 and 4800 cm^{-1}; optimized beam tuning resulted even in 9900 cm^{-1}. In the preceding Letter [3], the single-interaction condition (strictly only one photon absorbed and no other interactions) for the measurement of the relatively small triple-ionization cross section has been discussed in detail and unquestionably verified.

The photon flux was measured with a calibrated photodiode. The photon energy scale was calibrated with an uncertainty of better than ± 30 meV by remeasuring known photoionization resonances in C^{3+} [23]. Doppler shifts due to the ion velocity directed opposite to the incoming photons were corrected for, the correction factor of the laboratory photon energy being approximately 1.001. The systematic total uncertainty of the measured cross section for single and double ionization is $\pm 15\%$ [19], to which statistical uncertainties have to be added. In the case of triple ionization, the cross section was derived from ratios between consecutive recordings of the spectra for single, double, and triple ionization with the experimental conditions unchanged and by normalizing to the absolute data for single and double ionization. A conservative estimate of the uncertainty of the extremely small absolute triple-ionization cross section is $\pm 50\%$.

III. RESULTS

Figure 1 provides an overview of the investigated cross sections for single, double, and triple ionization of C$^+$ ions by single photons. Theoretical calculations for photoabsorption by ground-term and metastable C$^+$ ions [1] are displayed in Fig. 1(a). For metastable C$^+(1s^2 2s2p^2\ ^4P)$ ions with an excitation energy of about 5.33 eV [24], the available calculations are restricted to the energy range where $1s \rightarrow 2p$ excitations occur. The cross sections are represented by a black solid line with gray shading. For ground-term C$^+(1s^2 2s^2 2p\ ^2P)$ ions, the
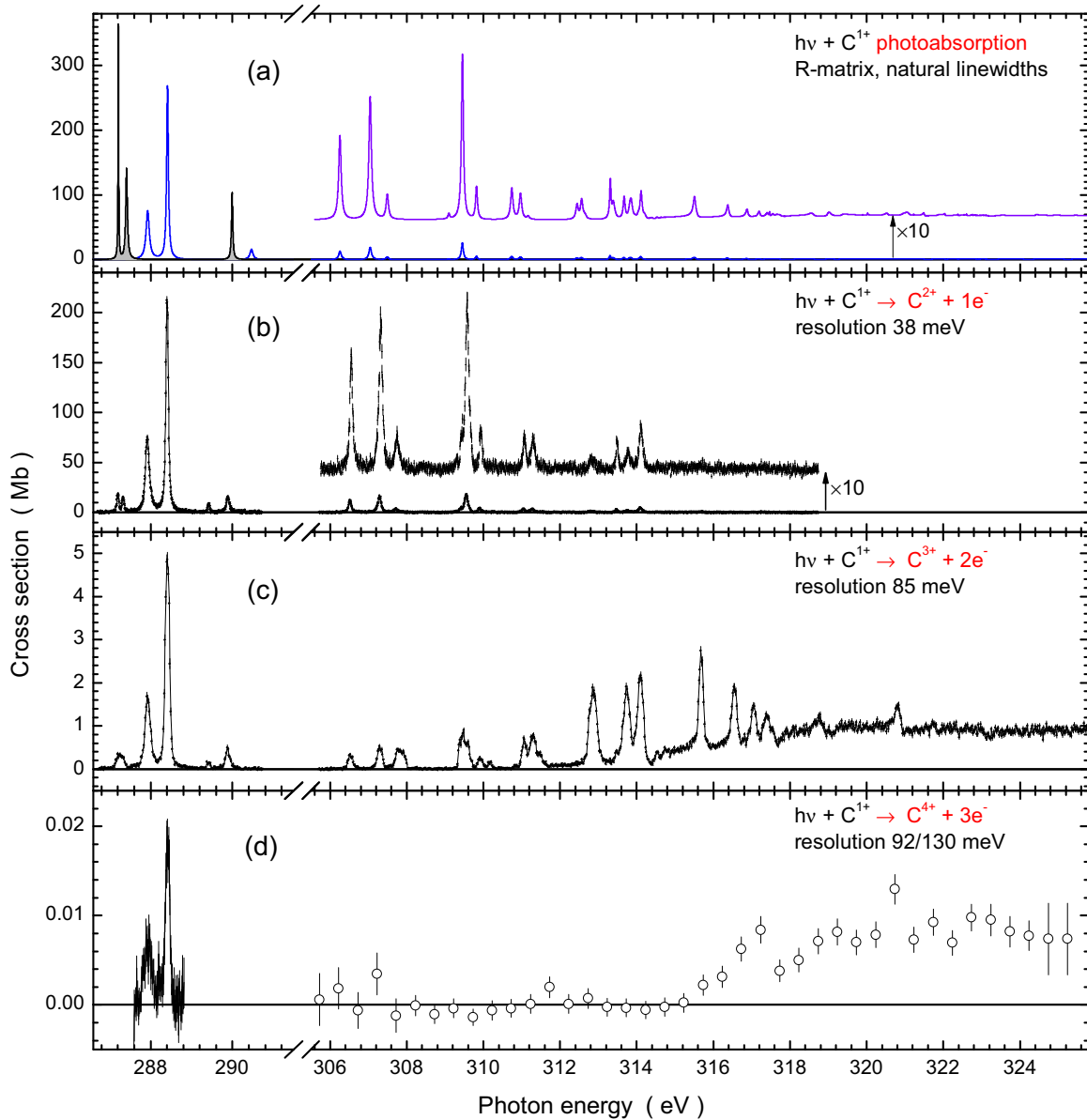
FIG. 1. Overview of the cross sections for photoionization of C^+ ions addressed in this paper. Panel (a) shows theoretical cross sections [1] for photoabsorption by long-lived excited $C^+(1s^2 2s 2p^2\ {}^4P)$ and ground-term $C^+(1s^2 2s^2 2p\ {}^2P)$ parent ions. The R-matrix results for the metastable ions are restricted to $1s \rightarrow 2p$ transitions. They are represented by the black solid line with gray shading. The calculated data for ground-term ions cover the full energy range 287–325 eV investigated in the present experiments. They are represented by the lighter (blue) solid line. Multiplication of the ground-term cross section by a factor of 10 produced the (purple) line, which is shown with a vertical offset for better visibility. The energy axis has a break between 294 and 305 eV, where no resonances are expected. Panel (b) displays experimental results for single photoionization of C^+ ions measured at an energy resolution of 38 meV. The cross sections obtained beyond 304 eV are shown a second time after multiplication by a factor of 10. They are displayed with an offset. All experimental cross sections are on an absolute scale. Panel (c) shows experimental results for double photoionization of C^+ ions measured at an energy resolution of 85 meV. In panel (d), cross sections for triple photoionization of C^+ ions are displayed. The densely spaced data at around 288 eV were measured at an energy resolution of 92 meV, and the data points with statistical error bars beyond 305 eV were taken at 130-meV resolution.

lighter (blue) solid line was calculated. Since the cross sections at energies beyond 305 eV are relatively small as compared to the $1s \rightarrow 2p$ resonances, they were multiplied by a factor 10 and displayed again in Fig. 1(a) with a vertical offset.

Figure 1(b) shows the experimental cross section for net single ionization of C^+ ions by single photons measured at a bandwidth of 38 meV. Like all other cross sections discussed in this paper, these data are on an independently absolute

scale. The spectrum at energies beyond 305 eV was multiplied by a factor of 10 and displayed again in Fig. 1(b) with a vertical offset for better visibility of the small resonance peaks. In Fig. 1(c), the experimental cross section for net double ionization of the C^+ ion by a single photon is displayed. It was measured at a bandwidth of 85 meV. The vertical scale is down from Fig. 1(b) by roughly a factor of 40. Figure 1(d) shows experimental cross sections for net triple ionization of
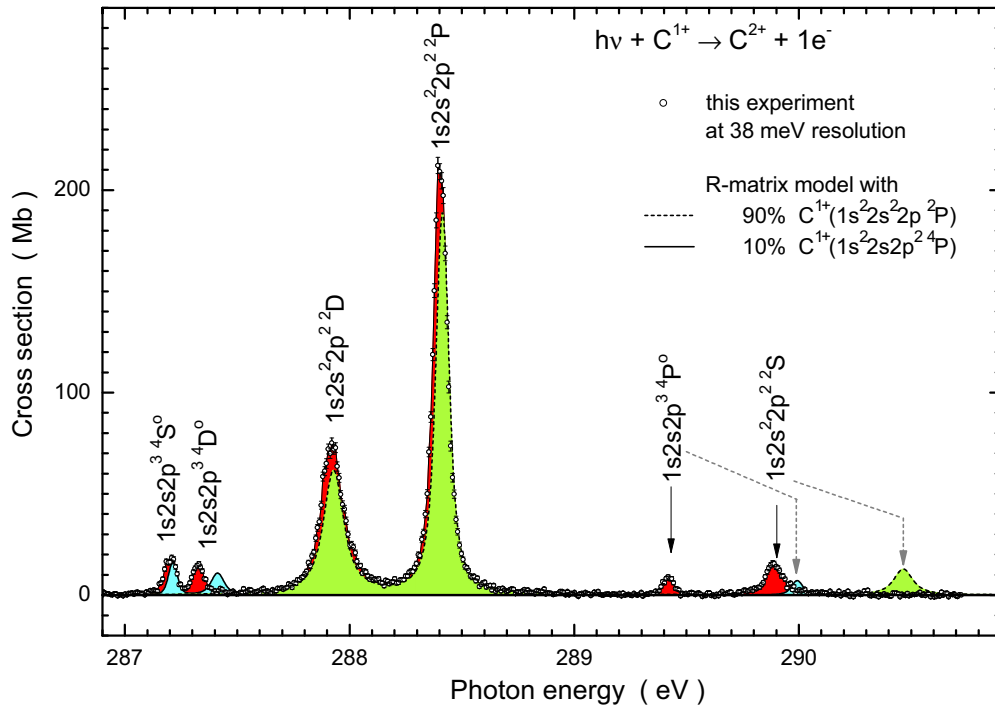
FIG. 2. Experimental cross section for single photoionization of C$^+$ ions in the region of $1s \rightarrow 2p$ excitations at 38-meV resolution compared with results of R-matrix photoabsorption calculations [1] convoluted with a 38-meV full-width-at-half-maximum (FWHM) Gaussian distribution function. The terms associated with the individual resonance peaks are indicated. The present measurement is represented by shaded circles with statistical error bars. The area under the experimental cross section is dark shaded (red online). The primary ion beam contained an approximate 10% fraction of metastable C$^+(1s^22s2p^2\,^4P)$ and 90% ground-term C$^+(1s^22s^22p\,^2P)$ ions. Accordingly, the R-matrix photoabsorption cross sections are a weighted sum of the different parent ion fractions which are individually presented: quartet resonances from metastable parent ions by a solid line with (cyan) shading and doublet resonances from ground-state ions by the dashed black line with (green) shading.

the C$^+$ ion by a single photon. The energy region around 288 eV was scanned in fine steps at a resolution of 92 meV. The isolated cross-section data at higher energies were measured at a bandwidth of 130 meV. Unfortunately, the low signal rates were not sufficient for scanning a wide energy range in small steps, so that resonance structures expected in the energy range 305–325 eV could not be made visible unambiguously. Note that the cross-section scale is down from that of Fig. 1(c) by another factor of about 200.

Figure 2 shows the result of a photon-energy scan at 38-meV resolution of the cross section for single photoionization of C$^+$ ions by single photons in the energy range 286.9–290.9 eV covering all contributions from $1s \rightarrow 2p$ excitations. Individual resonance terms are identified on the basis of the discussion provided in the work by Hasoğlu *et al.* [1]. The assignment of the first two peaks is reversed compared to earlier theoretical work [2,7]. Arguments for the new assignment are provided in the theory paper published by Hasoğlu *et al.* [1]. The quartet terms arise from metastable C$^+(1s^22s2p^2\,^4P)$ parent ions, and the doublet terms are populated by excitation of ground-level C$^+(1s^22s^22p\,^2P)$ ions. Both ground-state and metastable ions are present in the primary ion beam used in the experiments, as can be seen by comparing the cross sections displayed in Figs. 1(a) and 1(b) in the range of $1s \rightarrow 2p$ excitations.

Comparison of the ratios of experimental resonance strengths for the metastable and the ground-state components with the theoretical results obtained by Hasoğlu *et al.* [1], Wang and Zhou [7], as well as Shi and Dong [8] results in values

for the fractional abundance of metastable C$^+(1s^22s2p^2\,^4P)$ parent ions within $10 \pm 0.3\%$.

Figure 2 includes, as an example, the results of the R-matrix calculations carried out by Hasoğlu *et al.* [1] for both ion beam components. A weighted sum of the theoretical cross sections for 10% metastable and 90% ground-term components convoluted with a 38-meV FWHM Gaussian is compared with the experimental data. The theory data agree well with the experimental results for the dominant resonances. While peak areas are also predicted quite well for the smaller resonances, there are shifts of up to 0.5 eV in the calculated resonance energies for the $^4P^o$ and ^2S K-vacancy states. Previous R-matrix calculations [2] showed better agreement for the positions of the latter resonances but differed slightly in size and position for the strongest $(1s2s^22p^2\,^2P)$ resonance. Further comparisons of the experimental data with the theoretical cross sections mentioned above will be shown and discussed below.

The good agreement of the R-matrix photoabsorption calculations with the experimental cross sections for single ionization by single photons in the energy range 287–291 eV shows that photoabsorption in this energy range is dominated by K-shell excitations, $1s \rightarrow 2p$, of C$^+$ ions with subsequent single Auger decay populating the final C^{2+} product ion channel. This situation changes at higher photon energies, as Fig. 3 illustrates.

Figure 3 presents the comparison of theory and experiment at photon energies between 305 and 325 eV. Figure 3(a) shows the photoabsorption cross section calculated by Hasoğlu *et al.*
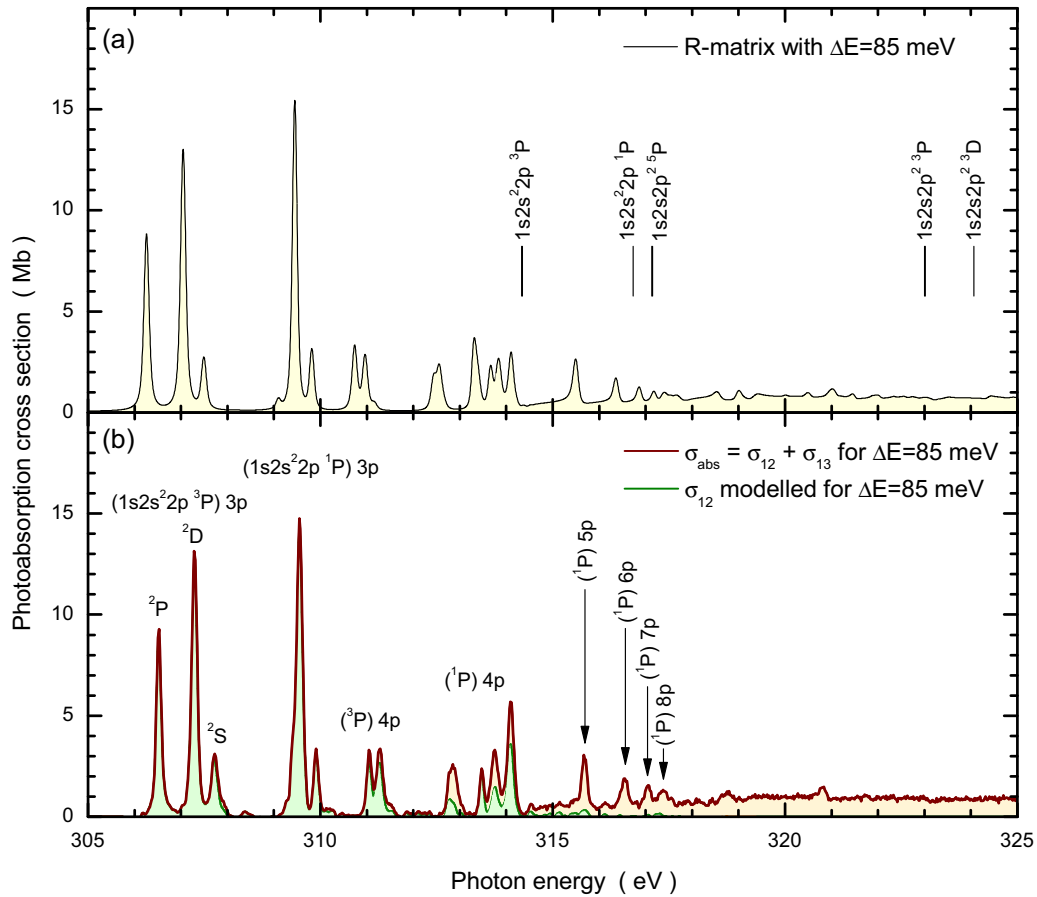
FIG. 3. Calculated and measured cross sections of C^+ ions interacting with photons in the energy range 305–325 eV. Panel (a) shows the theoretical cross section for photoabsorption by ground-state C^+ ions [1]. For comparison with the experimental results, in panel (b) the R-matrix results were convoluted with a 85-meV FWHM Gaussian. Energies of K-vacancy levels of C^{2+} ions relative to the ground level of C^+ were calculated by using the COWAN code and are indicated by vertical bars. The associated K-edge terms are also indicated. Panel (b) displays the experimentally derived cross section (see text) for single ionization of C^+ ions by single photons at 85-meV resolution represented by a thin (green) solid line with (light green) shading. The bold (brown) solid line with light (orange) shading represents the total experimental absorption cross section at 85-meV resolution. It is the sum of the experimental single and double photoionization cross sections at a photon beam bandwidth of 85 meV. Peak features in the spectrum have been identified by calculations using the COWAN code and, for the $1s2s^22p\ ^3P3p$ manifold, by the assignments provided by Sun *et al.* [25].

[1] convoluted with a 85-meV FWHM Gaussian distribution function [solid line with light (yellow) shading]. The lowest K-shell ionization thresholds relative to the $1s^22s^22p\ ^2P$ ground-state term of C^+ are indicated by vertical bars. They were calculated by using the COWAN code [26,27]. Computations with different sets of configurations showed substantial configuration interaction in the initial C^+ and K-shell ionized C^{2+} ions. Therefore, a relatively large set of configurations was used for the calculations of the K-shell ionization thresholds. For the initial C^+ ions, the following configurations were included: $1s^22s^22p$, $1s^22p^3$, $1s^22p3s^2$, $1s^22p3p^2$, $1s^22p3d^2$, $1s^22s^23p$, and $1s2s2p^3$. For the K-shell ionized C^{2+} ions, the set of configurations comprised $1s2s^22p$, $1s2p^3$, $1s2p3s^2$, $1s2p3p^2$, $1s2p3d^2$, $1s2s^23p$, and $2s2p^3$. In spite of the relatively large calculation, the resulting K edges may have uncertainties of the order of 1 eV. For example, the $1s2s^22p\ ^1P_1$ level which is the series limit of the $1s2s^22p(^1P)np$ Rydberg resonance series, clearly seen in both the theoretical and experimental spectra, should be near 317.6 eV rather than 316.7 eV as calculated with the COWAN code.

The GIPPER code [27] predicts the cross section for direct C^+ K-shell ionization to be about 0.8 Mb just above threshold, which is in fairly good agreement with the R-matrix calculation for photoabsorption and the experimental data for double ionization at energies beyond 319 eV. The K edges associated with $^3P_0$ (0.20 Mb), $^3P_1$ (0.40 Mb), and $^1P_1$ (0.20 Mb) constitute almost the full K-shell photoabsorption cross section, resulting from the R-matrix calculations at energies above the $^1P_1$ threshold.

Figure 3(b) displays the experimental cross section for single ionization of C^+ by a single photon as a thin (green) solid line with (light green) shading. There is remarkably good agreement of the experimental single-ionization cross section and the theoretical photoabsorption cross section at energies up to about 312 eV. With increasing photon energy, single ionization appears to die out and there is no sign of the K edge. Understanding this phenomenon is straightforward. When a K-shell electron is removed from C^+, the dominating reaction to be expected is an Auger decay of the resulting K-vacancy state in C^{2+} by which a further electron is removed and a C^{3+}

product ion is formed. Therefore, direct K-shell ionization results predominantly in net double ionization of the initial C^+ ion. Indeed, the associated cross-section function shows clear evidence of K edges at energies above approximately 314.3 eV.

With a much smaller probability, a double-Auger decay may follow the removal of a K-shell electron from C^+ producing C^{4+} and thus contributing to net triple ionization. This contribution is very small as evidenced by the results shown in Fig. 1(d). There is a clear signature of the K edge with a steep rise of the triple-ionization cross section at energies above 316 eV; however, the ionization continuum is about a factor 100 smaller than that in double ionization. As will be demonstrated below, radiative stabilization of a K vacancy in C^{2+} has a probability that is approximately two to three orders of magnitude smaller than that of Auger decay. Hence, photoabsorption by C^+ in the present energy range results almost exclusively in net single or double ionization. The sum of the associated cross sections σ_{12} and σ_{13}, respectively, is a very good approximation for the total photoabsorption cross section. Therefore, Fig. 3(b) includes that sum of the experimentally determined σ_{12} and σ_{13} at a photon energy bandwidth of 85 meV. It is represented by the bold solid (brown) line with (light orange) shading. Since single ionization was measured at 38-meV resolution and double ionization at 85-meV resolution, the experimental cross section σ_{12} was convoluted with a 76.03-meV FWHM Gaussian to model a resolution of 85 meV = $(38^2 + 76.03^2)^{1/2}$ meV before the two cross sections were added.

The experimentally derived cross section $\sigma_{abs} = \sigma_{12} + \sigma_{13}$ is in very satisfying agreement with the theoretical photoabsorption cross section. Only details in the structure far beyond the K edge appear to be somewhat different with two pronounced features in the experimental spectrum at about 318.7 and 320.8 eV, which are not as obvious in the theoretical result. One has to keep in mind in this context that the theory curve is for ground-state C^+ ions only, while the ion beam employed in the experiment included a 10% fraction of ions in metastable $1s^2 2s 2p^2\,^4P$ levels. Apparently, this beam contamination does not have a strong influence on the measured cross sections at energies beyond 305 eV.

The two features at 318.7 and 320.8 eV mentioned above [see also Fig. 1, highest-energy resonance peaks in Fig. 1(b)] have not been identified. Most likely, they are associated with double excitations in which a K-shell electron and an L-shell electron are simultaneously promoted by one absorbed photon. Identification of the most prominent resonance features in the photoabsorption spectra is complicated by the very large number of levels that can potentially contribute. Again the GIPPER code [27] was employed to see how much absorption oscillator strength is contributed by which levels at which excitation energies. Given the uncertainty of the calculated energies a level-by-level identification was not attempted.

For the calculations, a large set of configurations was included: $1s^2 2s^2 2p$, $1s^2 2p^3$, $1s^2 2p 3s^2$, $1s^2 2p 3p^2$, $1s^2 2p 3d^2$, $1s^2 2s^2 3p$, $1s 2s 2p^2 np$, $1s 2s 2p^2 ns$, $1s 2s^2 2p np$, $1s 2p^3 np$, with $n = 2, 3, \ldots, 9$ and $1s 2s 2p^2 nd$, with $n = 3, 4, \ldots, 9$. More than 9000 transitions were considered and their dipole oscillator strengths f_a for absorption calculated. Because of the uncertainties of the calculated resonance energies, the relative positions of K-shell excited levels and the magnitude of the

oscillator strengths were used to assign configurations to the most prominent peak features in the spectrum. According to this analysis, the energy range 306–308 eV is dominated by levels in the $(1s 2s^2 2p\,^3P)3p$ manifold, the range 309–310.5 eV by levels in the $(1s 2s^2 2p\,^1P)3p$ manifold, and the range 310.5–312 eV appears to be due to $(1s 2s^2 2p\,^3P)4p$ levels. The Rydberg series of $(1s 2s^2 2p\,^3P)np$ resonances converges to the $1s 2s^2 2p\,^3P$ K-shell ionization edge at about 314.5 eV and is buried under resonances associated with $(1s 2s^2 2p\,^1P)4p$ levels. The $(1s 2s^2 2p\,^1P)np$ Rydberg sequence with $n = 5, 6, 7, 8, \ldots$ dominates in the energy range 315.5–317.8 eV.

Figures 2 and 3 demonstrate that the K-shell excited levels of C^+ in the energy range up to about 312 eV predominantly decay by emission of one electron. These levels are associated with $1s \to 2p$, $1s \to 3p$, and partly with $1s \to 4p$ excitations. When the principal quantum number of the outermost excited electron increases further, the probability for the emission of two electrons increases and the final product is a C^{3+} ion. At energies beyond the $1s 2s^2 2p\,^3P$ K-shell ionization threshold, even the resonantly excited C^+ ions decay almost exclusively by two-electron emission. As a result, the cross section for absorption of a photon by a C^+ ion in that energy range is nearly identical with the cross section for net double ionization.

The present experiment with its low detector background and its high photon flux provided much better conditions than those faced in the experiments of Schlachter *et al.* [2] on K-shell excitation followed by single-Auger decay at the Advanced Light Source (ALS) in Berkeley. Hence, it was possible to increase the resolving power by approximately four times that of the previous experiment. The smallest photon energy bandwidth reached by Schlachter *et al.* was 50 meV. At this bandwidth, only the two strongest resonances in the spectrum could be measured with moderate statistics. Compared to the previous best resolution, the bandwidth was reduced in the present experiment to about one fourth. The complete spectrum of $1s \to 2p$ resonances of C^+ ions in the energy range 286.5–290.5 eV was measured at a resolution of 12 meV. The resulting high-resolution cross section for single ionization of C^+ ions is shown in Fig. 4(b) together with a 38-meV resolution measurement in Fig. 4(a) in which excellent statistical precision was reached.

From the experimental results displayed in Fig. 4, resonance parameters for all the six peaks related to $1s \to 2p$ excitations can be extracted using a global fit to both spectra. However, one has to consider that all the K-shell excited levels are multiplets, as are the initial electronic levels of the parent C^+ ions. Because of the natural widths of the excited levels, none of these multiplets can be resolved in an experiment, even at infinite resolving power. The electron-cyclotron-resonance ion source used in the present experiments is known to produce a plasma with high electron temperatures. Therefore, it is easily possible to ionize and excite ions in a wide range of charge states. Excited states of ions with sufficiently long lifetimes can survive the time between their population in the plasma and the extraction of the ions from the source. They can further survive the time of flight between the source and the photon-ion interaction region, which was about $30\,\mu s$ in the present case of C^+ ions. Candidates for such survival are the
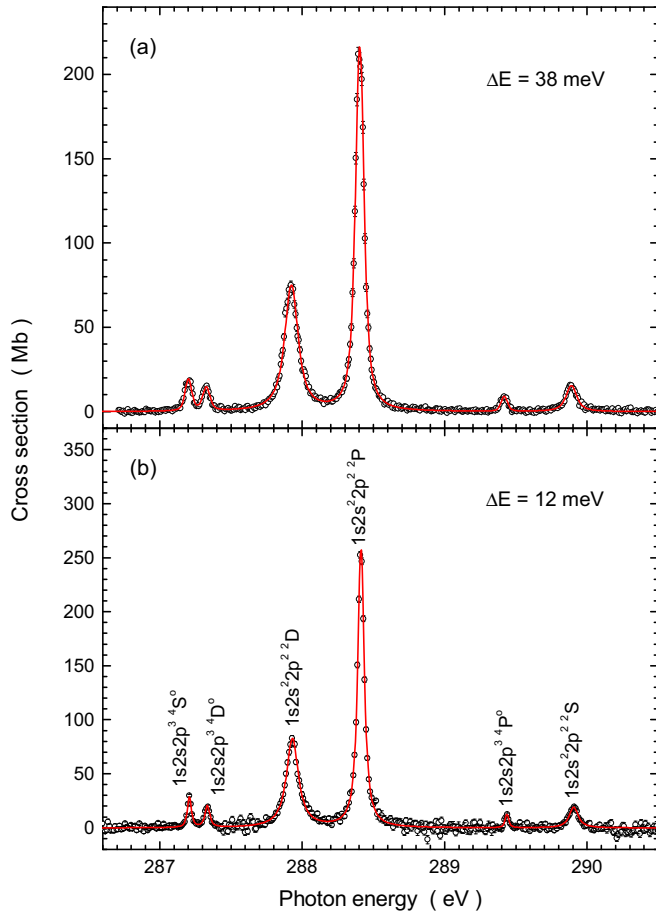
FIG. 4. Measured cross sections for net single ionization of C$^+$ ions measured at resolution 38 meV (a) and 12 meV (b). The parent ion beam contained 10% metastable ^4P and 90% ^2P ground-term ions. The solid (red) lines are fits to the two spectra as described in the main text.

first four excited electronic (fine-structure) levels associated with the $1s^2 2s^2 2p\ ^2P^\mathrm{o}$ ground term and the energetically lowest metastable $1s^2 2s 2p^2\ ^4P$ term.

The NIST Atomic Spectra Database [24] provides the following energies for the relevant levels populated by the ions in the parent ion beam: 0.00000 eV ($^2P^o_{1/2}$), 0.007863 eV ($^2P^o_{3/2}$), 5.33173 eV ($^4P_{1/2}$), 5.33446 eV ($^4P_{3/2}$), and 5.33797 eV ($^4P_{5/2}$). So the possible initial terms feature fine-structure splitting by up to almost 8 meV. The $1s \rightarrow 2p$ excited terms in Fig. 4 are $1s2s^2 2p^2\ ^2D, ^2P, ^2S$ and $1s2s2p^3\ ^4S^\mathrm{o}, ^4D^\mathrm{o}, ^4P^\mathrm{o}$. According to Shi and Dong [8], the fine-structure splitting within the ^2D term is 12 meV and it is 13 meV within the ^2P term. Similar splittings are found for the K-shell excited quartet terms.

Selection rules for electric dipole transitions between the initial and final terms limit the number of possible transitions between the initial and final levels. Nevertheless, the six peaks observed in the experiment in the energy range 287–291 eV comprise 27 significantly contributing level-to-level transitions [8]. The ^2D resonance populated from the ground term is made up of three transitions with transition energies differing by up to 19 meV. The ^2P resonance comprises four transitions separated by a maximum of 21 meV and the ^2S peak consists

of two transitions separated by 8 meV. Similarly, the three peaks in the quartet system populated by excitation of ions initially in one of the $1s^2 2s 2p^2\ ^4P$ levels are composed of 18 levels in total. The $^4S^\mathrm{o}$ resonance consists of three lines separated by a maximum of 3 meV. The $^4D^\mathrm{o}$ peak contains eight lines separated by a maximum of 14 meV and the $^4P^\mathrm{o}$ peak comprises seven transitions separated by a maximum of 9 meV. All the fine-structure splittings given above were taken from the theoretical results obtained by Shi and Dong [8].

The multiplet structure complicates the interpretation of linewidths obtained by theory and experiment. In previous work addressing K-shell excitation of B-like ions C$^+$ [2], N^{2+} [9], and O^{3+} [10], the multiplet nature of the resonances was not considered. Not accounting for the fine-structure effects is acceptable as long as the level splitting is much smaller than the natural or lifetime width Γ of the individual transitions. This has to be investigated for each case. Without further discussion of fine-structure splitting, the Lorentzian width Γ_L extracted from resonance fits has to be interpreted as an effective natural width, which is not necessarily identical with the lifetime width.

In order to quantify the possible effects of fine-structure splittings on the widths of the $1s \rightarrow 2p$ photoexcitation resonances, the information on resonance energies, natural line widths, and oscillator strengths provided by Shi and Dong [8] for each of the 27 possible $1s \rightarrow 2p$ resonance transition was used to construct a suitable model for fitting the experimental photoionization cross section. By careful inspection of Table III of their publication, it became apparent that they had entered wrong numbers for the oscillator strengths for the three transitions $^4P^o_{5/2} \rightarrow {}^4S_{3/2}$, $^4P^o_{3/2} \rightarrow {}^4S_{3/2}$, and $^4P^o_{1/2} \rightarrow {}^4S_{3/2}$. The corrected numbers [28] are 0.577, 0.404, and 0.186, respectively. The gf values calculated in length form were divided by the statistical weights of the $^4P^\mathrm{o}$ initial levels and then the resonance strengths were calculated for each combination of initial levels $|i\rangle$ to final levels $|k\rangle$ from the formula (see the Appendix)

$$S = \int_{E_\gamma} \sigma_\mathrm{tot}(E_\gamma)\, dE_\gamma = f_{ik} \times 109.761\ \mathrm{Mb\,eV}, \quad (1)$$

where E_γ is the photon energy and σ_{tot} is the cross section for total photoabsorption via the $|i\rangle \rightarrow |k\rangle$ transition. The quantity f_{ik} is the oscillator strength of that transition.

The six apparent peak features were then fitted by 27 Voigt profiles, each of which is characterized by a Lorentzian and a Gaussian width, the resonance energy, and the resonance strength. In addition, a constant background cross section was allowed. Rather than using a 109-parameter fit, a number of constraints were introduced. The Gaussian widths characterizing the experimental energy spread are all the same for each of the 27 profiles within one measured spectrum. Furthermore, the Lorentzian widths associated with each of the fine-structure levels of one term have been assumed to be identical. Only the six energies of the lowest-energy transitions within each of the six apparent resonance features were used as fit parameters while the remaining transition energies were fixed by the fine-structure splittings calculated by Shi and Dong [8]. Also, only six parameters were used to fit the 27 resonance strengths by keeping the calculated relative resonance strengths within

TABLE I. Parameters characterizing the $1s \to 2p$ excitation resonances associated with ground-state $C^{+}(1s^2 2s 2p\ ^2P)$ (first three columns) and metastable $C^{+}(1s^2 2s 2p^2\ ^4P)$ parent ions (last three columns). The top entry of each column is the K-vacancy term excited by a single photon. The resonance energies E_{res} are given with three decimals because their relative uncertainties are of the order of only 5 meV. The absolute calibration uncertainty is 30 meV. Throughout this paper, the numbers in round brackets following a measured quantity denote the uncertainty of the last digits. The following parameters are provided as extracted from resonance fits to the measured spectra: E_{res}, the resonance energy relative to the initial term energy; Γ_L, the Lorentzian width of the excited level; S_{1e}, the partial resonance strength for net single ionization; S_{2e}, the partial resonance strength for net double ionization; S_{3e}, the partial resonance strength for net triple ionization; λ, the transition wavelength; τ, the lifetime of the excited level; S, the total resonance strength for photoabsorption; f_{ik}, the oscillator strength for absorption from level $|i\rangle$ to level $|k\rangle$; A_{ki}, the associated Einstein coefficient for radiative decay of the excited level; Γ_γ, the radiative (partial) width of the excited level; Γ_{1e}, the partial width for the emission of one electron; Γ_{2e}, the partial width for the emission of two electrons; Γ_{3e}, the partial width for the emission of three electrons; A_{1e}, the single-Auger decay rate; A_{2e}, the double-Auger decay rate; and A_{3e}, the triple-Auger decay rate. Quantities (S_{1e}, S_{2e}, S_{3e}, and S) that depend on the fraction of ions in the specified initial term are normalized to a fraction of 100% so that the derived parameters (such as f_{ik}) retain their intended meaning.

Parameter	$1s2s^2 2p^2\ ^2D$	$1s2s^2 2p^2\ ^2P$	$1s2s^2 2p^2\ ^2S$	$1s2s2p^3\ ^4S^o$	$1s2s2p^3\ ^4D^o$	$1s2s2p^3\ ^4P^o$
E_{res} [eV]	287.931(30)	288.413(30)	289.906(30)	287.208(30)	287.334(30)	289.437(30)
Γ_L [meV]	101(3)	49(2)	70(5)	24(3)	37(4)	22(5)
S_{1e} [Mb eV]	14.6(2.2)	23.8(3.6)	2.48(40)	13.4(4.0)	12.6(3.8)	5.46(1.7)
S_{2e} [Mb eV]	0.38(6)	0.81(13)	0.084(13)	0.36(11)	0.34(10)	0.15(5)
S_{3e} [Mb eV]	0.0019(10)	0.0032(16)				
λ [nm]	4.30604(45)	4.29884(45)	4.27670(44)	4.31688(45)	4.31499(45)	4.28363(44)
τ [fs]	6.5(2)	13.4(5)	9.4(7)	27.4(3.4)	17.8(2.4)	29.9(6.8)
S [Mb eV]	15.0(4.1)	24.9(7.0)	2.57(91)	14.3(7.7)	13.0(7.1)	5.65(3.4)
f_{ik}	0.137(38)	0.227(64)	0.0234(83)	0.130(71)	0.118(65)	0.051(31)
A_{ki} [10^{11} s^{-1}]	2.95(81)	8.18(2.3)	2.56(91)	14.0(7.6)	2.54(1.4)	1.9(1.1)
Γ_γ [meV]	0.19(6)	0.54(15)	0.17(6)	0.92(50)	0.17(9)	0.12(7)
Γ_{1e} [meV]	98.3(10.0)	46.9(5.1)	67.6(8.3)	22.5(3.6)	35.9(6.0)	21.3(5.3)
Γ_{2e} [meV]	2.5(3)	1.6(2)	2.3(3)	0.61(10)	0.95(16)	0.60(15)
Γ_{3e} [meV]	0.013(7)	0.0063(32)				
A_{1e} [10^{13} s^{-1}]	14.9(1.6)	7.1(8)	10.3(1.3)	3.4(6)	5.5(1.0)	3.2(8)
A_{2e} [10^{11} s^{-1}]	38.5(4.0)	24.4(2.6)	34.6(4.3)	9.2(1.5)	14.5(2.4)	9.1(2.3)
A_{3e} [10^{9} s^{-1}]	19(10)	9.6(5.0)				

each peak feature identical to those predicted by theory [8]. With all these constraints, the Gaussian width, six Lorentzian widths, six apparent resonance energies, and six factors for correcting the theoretical resonance strengths were extracted from the experiment.

The resulting parameters for the six $1s \to 2p$ excitation resonances are provided in Table I. The first row shows the excitation energies found for the six resonances. Their absolute calibration uncertainty is ± 30 meV. Yet the energies are given with three decimals because the relative uncertainty is less than 5 meV. The second and third rows show the remaining parameters resulting from the fit of the spectra in Fig. 4, i.e., the natural line widths $\Gamma = \Gamma_L$ and the resonance strengths S_{1e} for one-electron removal. The estimated uncertainties are given by the numbers in brackets. In similar fits to experimental spectra (see Figs. 1 and 6), the resonance strengths S_{2e} for two-electron removal, and S_{3e} for three-electron removal were also determined. The measured strengths were normalized to 100% considering the relative fractions of ions in the ground term (90%) and the metastable term (10%) in the measurement. In other words, the resonance strengths obtained from the measurements were divided by 0.9 in case of the resonances populated from the ground-state term and by 0.1 in the case of resonances populated from the metastable parent ion term.

The remaining parameters provided in Table I have all been derived from the observables given in the first five rows. The relevant formulas are collected in the Appendix, which describes the procedure used for extracting all the additional information about the observed resonances. For convenience, the sixth row of Table I shows the wavelength of the transitions observed in the experiment. These are readily obtained from Eq. (A5). The lifetimes of the core-excited terms are easily calculated from Eq. (A6). The determination of the resonant-absorption strength S is more involved and requires additional information about radiative transition rates. An iterative procedure which converges after two steps provides S and the oscillator strength f_{ik} as well as the radiative decay rate A_{ki} and the partial width Γ_γ for radiative decay of the core-excited term. Following from these parameters and the measured resonance strengths S_{ne} ($n = 1, 2, 3$) for the removal of n electrons, the transition rates A_{ne} for single-, double-, and triple-Auger decay as well as the partial widths of these decays can also be obtained.

The information collected in Table I can be used for constructing the natural (unconvoluted) absorption cross section related to $1s \to 2p$ excitation of C^+. This can be directly compared to the results of theoretical calculations. In principle, for such comparisons the cross sections for exclusively ground-term C^+ ions can be separated from the cross sections for exclusively metastable C^+ ions. Instead, comparisons are made assuming the conditions of the present experiment, i.e., 10% metastable and 90% ground-level ions. The experimentally
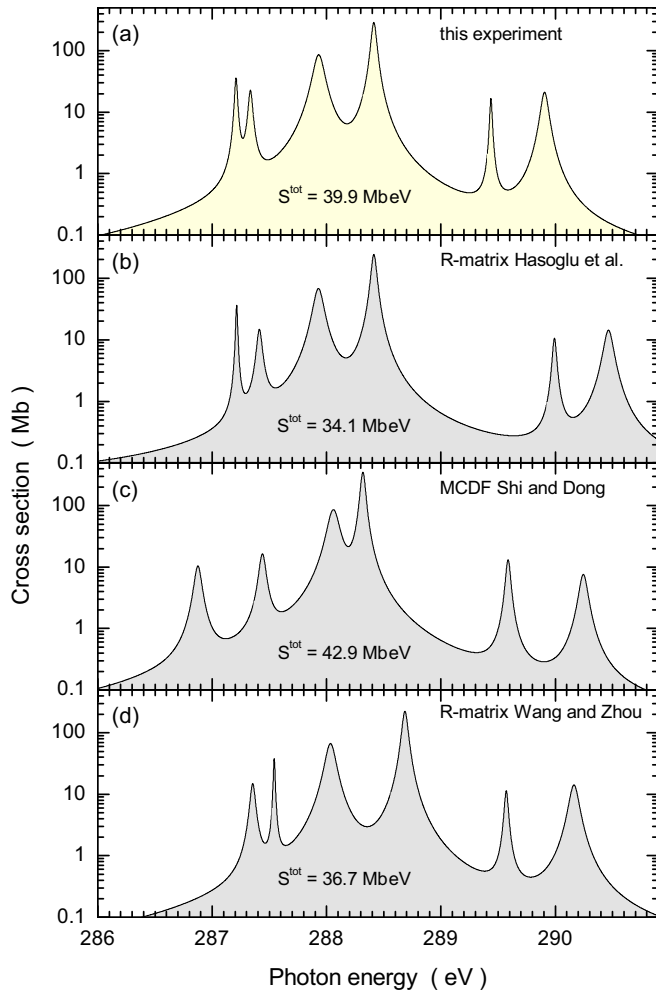
FIG. 5. Natural-line-width absorption cross sections of C^+ determined by the present experiment with a 90% fraction of ^2P ground level and 10% of ^4P metastable ions in the parent ion beam. The experimental spectrum (a) is compared with calculations by Hasoğlu *et al.* [1] (b), Shi and Dong [8] (c), and Wang and Zhou [7] (d). The theory spectra were modeled assuming the experimental distribution of ground-term and metastable ions. Each panel displays the total resonance strength S^{tot} contained in the associated photoabsorption spectrum.

derived natural cross section for such a mixture is shown in Fig. 5(a).

The simulated experimental cross section is compared with the results of two *R*-matrix calculations [1,7] and the cross section reconstructed from the detailed information provided by Shi and Dong on the basis of their multiconfiguration Dirac-Fock calculations [8]. All cross sections are shown on a logarithmic scale to emphasize the smaller resonances in the comparison. The calculations show spectra which are quite similar to the experimental result. Obvious differences are mainly in the positions of the six resonance features. However, one has to keep in mind that the deviations are typically only within several tens of meV and reach no more than about 550 meV in a few cases. Such deviations at level energies of approximately 290 eV are less than 0.19%.

In Fig. 5, the total resonance strength of each spectrum is provided. The average of the theoretical resonance strengths is 37.9 Mb eV, which is only 9.5% from the experimental value. The maximum deviation is 14.5% which is still within the experimental uncertainty. While the resonance energies and the peak areas in the theory spectra are close to the experiment there are dramatic differences in the peak widths between different theoretical approaches and between theory and experiment. Quantitative comparisons are provided in Table II where selected parameters listed in Table I are compared with theoretical and experimental data available in the literature.

The parameters for which comparisons are possible are the resonance energies E_{res}, the oscillator strengths f_{ik}, the natural width Γ which is equal to the Lorentzian width Γ_L found in the fits, the radiative decay rate A_{ki}, and the single-Auger decay rate A_{1e}.

The resonance energies found in the present investigation agree with most of the other experimental findings within their error bars. Deviations are observed for the positions of the smaller peaks in the spectrum, particularly when comparing with the spectroscopic work of Jannitti *et al.* [4]. Differences with theoretical calculations have already been discussed and are below a level of 1.90×10^{-3}.

The experimentally derived oscillator strengths for absorption have estimated uncertainties between 28% for the strongest ground-term resonances and about 60% for the resonances associated with metastable parent ions. The reason for the relatively large error bars is in the uncertainty of the 10% fraction of the metastable component in the parent ion beam. With only few exceptions, the theoretical oscillator strengths are well within the experimental error bars.

With an instrumental width of only 12 meV, the determination of natural line widths for core-excited levels of C^+ ions can be expected to be quite accurate. Compared to the previous experiment by Schlachter *et al.* [2], the uncertainties of some of the Γ values could be substantially reduced by factors up to 8. Nevertheless, the width of the broadest resonance, associated with the core-excited ^2D term, is within 4% in both experiments. In other cases, the uncertainties quoted in the earlier experiment were slightly too optimistic. The theoretical natural widths show substantial scatter by factors up to about 5. On average, theory predicts broader resonances for metastable parent ions than what the experiment yields.

The radiative decay rates derived from the present experiment can be directly compared with the calculations by Sun *et al.* [25], who used the saddle-point variation and complex-rotation methods including relativistic and mass polarization corrections in first-order perturbation theory. The calculated radiative transition rates are in agreement with the experiment within the experimental uncertainties. Finally, the total transition rates for single-Auger decay found by the present measurement are compared with the results of four different theoretical calculations. For the resonances associated with ground-term parent ions, theory and experiment are in quite satisfying agreement. However, in a few cases there are deviations exceeding a factor of 2.

The comparisons show that the accurate calculation of atomic transition parameters for a relatively simple atomic ion with only five electrons is still a challenge. With the results obtained in the present experiment for double- and triple-Auger

TABLE II. Selected parameters from Table I in comparison with experimental and theoretical results for the $1s \rightarrow 2p$ excitation resonances associated with ground-state $C^+(1s^2 2s^2 2p\ ^2P)$ (first three columns) and metastable $C^+(1s^2 2s 2p\ ^4P)$ parent ions (last three columns). The peak assignment by Schlachter *et al.* [2] as well as that by Wang and Zhou [7] have been corrected according to the discussion by Hasoğlu *et al.* [1] and the results of Shi and Dong [8]. The calculations by Shi and Dong are differential in the total angular momentum and appropriately weighted sums were entered into this table.

Parameter	$1s2s^2 2p^2\ ^2D$	$1s2s^2 2p^2\ ^2P$	$1s2s^2 2p^2\ ^2S$	$1s2s2p^3\ ^4S^o$	$1s2s2p^3\ ^4D^o$	$1s2s2p^3\ ^4P^o$
E_{res} [eV]						
Experiment						
This work	287.931(30)	288.413(30)	289.906(30)	287.208(30)	287.334(30)	289.437(30)
[2]	287.93(3)	288.40(3)	289.90(3)		287.25(3)	289.42(3)
[4]	287.91(7)	288.59(7)	289.95(7)	287.09(7)	288.02(7)	289.80(7)
Theory						
[1] Spectrum fit	287.929	288.414	290.465	287.213	287.413	289.992
[1] Their Table I	287.966	288.303	290.279	286.997	287.465	290.012
[8]	288.061	288.317	290.240	286.875	287.440	289.587
[7]	288.034	288.685	290.163	287.354	287.542	289.571
[25]	287.90	288.56	289.92		287.33	289.63
[2]	287.96	288.63	289.97	287.29	287.73	289.46
f_{ik}						
This work	0.137(38)	0.227(64)	0.023(8)	0.13(7)	0.12(7)	0.051(31)
Theory						
[1] Spectrum fit	0.100	0.191	0.020	0.084	0.095	0.053
[8] Length form	0.139	0.249	0.028	0.002[a]	0.132	0.079
[8] Velocity form	0.126	0.226	0.025	0.002[a]	0.125	0.074
[8] Revised				0.0973[a]		
[7] Length form	0.1015	0.1927	0.0197	0.0968	0.0844	0.0547
[7] Velocity form	0.0977	0.1855	0.0194	0.0931	0.0812	0.0534
Γ [meV]						
Experiment						
This work	101(3)	49(2)	70(5)	24(3)	37(5)	22(5)
[2]	105(15)	59(6)	112(25)		110(40)	55(25)
Theory						
[1] Spectrum fit	94	50	87	16	47	36
[8]	101	43	77	57	67	42
[7]	96	54	88	47	16	35
[2]	103	62	93	25	84	52
A_{ki} [10^{11} s^{-1}]						
Experiment						
This work	2.95(81)	8.18(2.3)	2.56(91)	14.0(7.6)	2.5(1.4)	1.9(1.1)
Theory, length form						
[25]	2.25	6.98	2.24		3.22	1.91
A_{1e} [10^{13} s^{-1}]						
Experiment						
This work	14.9(1.6)	7.12(77)	10.3(1.3)	3.42(55)	5.45(92)	3.23(80)
Theory, length form						
[29]	13.1	7.22	12.6	8.90	7.25	5.67
[1]	13.9	7.49	13.1	2.35	6.99	5.41
[30]	17.6	7.88	15.5	3.13	9.75	7.40
[8]	15.4	6.44	11.7	10.1	8.53	6.29

[a]Entries in Table III of reference [8] are most likely misprinted; the corrected number, 0.0973, was calculated by Shi and Dong [28] using the FAC code.

decays, the challenge becomes even greater. Theoretical attempts are being developed to deal with multielectron ejection subsequent to inner-shell excitation (see, e.g., Ref. [16]). However, so far only one calculation has been published addressing the multielectron, and particularly the triple-Auger decay processes associated with K-shell excitations of C^+ ions that have been studied in the present experiment. But very

encouraging theoretical work that includes calculations also of direct triple-Auger decay is under way [31].

The last part of this paper is devoted to the quantitative description of multiple ionization of C^+ ions as the result of the absorption of a single photon. For the strongest resonances found in single ionization, additional measurements of single, double, and triple ionization were carried out at a fixed energy
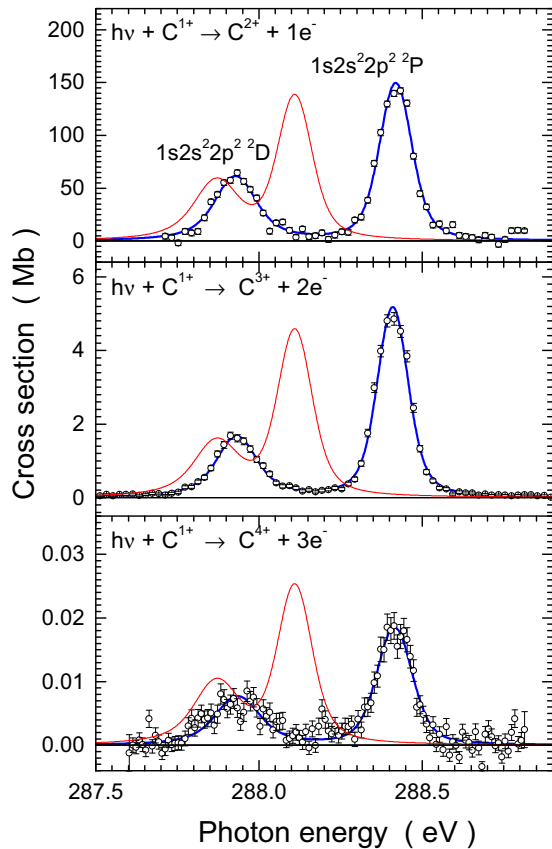
FIG. 6. Cross section for single, double, and triple ionization of ground-state C^+ ions by single photons at 92-meV bandwidth. The resonances seen in all the observed channels are associated with K-shell-excited $C^+(1s2s^22p^2\ ^2D,\ ^2P)$ terms. The dark solid (blue) lines represent the fits to the experimental spectra with Voigt profiles from which Auger decay probabilities were obtained. The light (red) solid lines show theory-based absolute cross sections derived from calculations of single-, double-, and triple-Auger decay rates by Zhou *et al.* [32]. For details, see main text.

TABLE III. Comparison of the present resonance parameters for $C^+(1s^22s^22p\ ^2P) \rightarrow C^+(1s2s^22p^2\ ^2D,\ ^2P)$ excitations with calculations by Zhou *et al.* [32], including the triple-Auger decay rate. The data obtained by Zhou *et al.* were taken from their Table I for A_{1e} and derived from the ratios given in their Table IV.

Parameter	$1s2s^22p^2\ ^2D$	$1s2s^22p^2\ ^2P$
E_{res} [eV], this work	287.931(30)	288.413(30)
E_{res} [eV], Zhou *et al.*	287.87	288.11
Γ [meV], this work	101(3)	49(2)
Γ [meV], Zhou *et al.*	114	57
A_{1e} [10^{13} s^{-1}], this work	14.9(1.6)	7.1(8)
A_{1e} [10^{13} s^{-1}], Zhou *et al.*	17.4	8.66
A_{2e} [10^{11} s^{-1}], this work	38.5(4.0)	24.4(2.6)
A_{2e} [10^{11} s^{-1}], Zhou *et al.*	53.4	27.1
A_{3e} [10^{9} s^{-1}], this work	19(10)	9.6(5.0)
A_{3e} [10^{9} s^{-1}], Zhou *et al.*	31.2	15.8

for single, double, and triple ionization of $C^+(1s^22s^22p\ ^2P)$ ions by a single photon via excitation of K-shell excited $C^+(1s2s^22p^2\ ^2D,\ ^2P)$ terms. For producing absolute cross sections additional information on the absorption oscillator strength is required which has not been provided by Zhou *et al.* By using the experimentally derived values of f_{ik} (see Table II) plus the parameters calculated by Zhou *et al.* as presented in Table III the light (red) solid curves in Fig. 6 have been computed which represent the absolute cross sections for single (upper panel), double (middle panel), and triple (lower panel) ionization of C^+. For direct comparison with the experiment, the theoretical cross sections were convoluted with 92-meV FWHM Gaussians.

The resonance energies obtained by Zhou *et al.* are slightly off; however, the differences are at most 300 meV corresponding to 0.1% of the associated resonance energies. The magnitudes of the cross sections, partly being adjusted to the experimental data by using the experimentally derived oscillator strengths, give remarkable agreement for all three final-charge states of the ionized ions, which requires realistic multielectron-ejection decay rates. The comparison of these rates in Table III shows a level of agreement that is very encouraging for further developments in this field of research.

IV. SUMMARY

In this paper, which is a followup to a previous Letter [3], details of the experiments are presented. In particular, the experimental data are compared to available theoretical results from different computational approaches. From high-resolution absolute cross-section measurements at a resolving power of up to 24 000, exceeding that of previous experiments by a factor of 4, complete sets of transition parameters for $1s \rightarrow 2p$ excitations of ground-term and metastable C^+ ions could be derived. These include not only the resonance energies, natural widths, and resonance strengths but also the transition rates for radiative decay as well as single-, double-, and triple-Auger decays. Oscillator strengths, partial decay widths, transition wavelengths, and lifetimes of K-shell excited terms are also readily computed from the extracted information. Comparison of these quantities with data available in the literature show

resolution of 92 meV [3]. The lowest panel in Fig. 6 shows the unambiguous observation of C^{4+} product ions arising from K-shell excited $C^+(1s2s^22p\ ^2D,\ ^2P)$ states which are populated from the ground-state term of C^+ via one-photon absorption $\gamma + C^+(1s^22s^22p\ ^2P) \rightarrow C^+(1s2s^22p^2\ ^2D,\ ^2P)$. The resulting K-vacancy states can obviously decay by the emission of up to three electrons. Other conceivable explanations for the observation of C^{4+} product ions such as two-photon absorption or one-photon absorption plus one or more interactions with residual-gas particles were discussed in our previous Letter [3] and shown to be negligible.

Along with the experimental data, Fig. 6 presents theoretical cross-section curves constructed from calculations of single-, double-, and triple-Auger decay of K-shell excited $C^+(1s2s^22p^2\ ^2D,\ ^2P)$ terms. Decay rates for Auger processes starting from these terms with emission of one, two, or three electrons were computed by Zhou *et al.* [32] and are compared in Table III with the experimentally derived decay rates. From the theoretical decay rates as well as the calculated resonance energies E_{res} and natural widths Γ, also provided in Table III, relative theoretical cross sections can be constructed

mixed agreement. This is remarkable since C^+ with only five electrons is a relatively simple system. It is all the more encouraging that now also the decay rates for multielectron ejection up to the triple-Auger decay can be theoretically accessed, producing results that are in remarkable agreement with the present measurements and opening a new window into the important field of many-electron processes in atomic systems.

APPENDIX: DETERMINATION OF ATOMIC TRANSITION RATES AND RELATED QUANTITIES FROM ABSOLUTE HIGH-RESOLUTION CROSS-SECTION MEASUREMENTS OF PHOTOIONIZATION RESONANCES

This Appendix introduces quantities often used in atomic and molecular spectroscopy and provides information on their mutual relations. Such information can be found in textbooks and scientific papers (see, for example, [26,33–35]). However, the use of different definitions such as line strength and resonance strength may cause confusion. Moreover, different unit systems in theoretical treatments and in the resulting equations provide additional pitfalls. It is felt, therefore, that a consistent set of spectroscopic quantities and equations should be introduced and discussed in the present context. In all formulas, SI units are used. On the basis of the relations provided in the following, many of the data presented in this paper have been derived.

Photoionization of an atom or an ion can proceed in a direct process in which an electron is removed from one of the occupied subshells. Alternatively, an inner-shell electron can be excited to an autoionizing state that relaxes by Auger decay. The latter process is characterized by a resonance in the cross section which is associated with the intermediate multiply excited state. This state has an intrinsic width, the natural width Γ, and is found at the photon energy $E_{\rm res}$. This energy is required to populate the intermediate excited level from the initial state which can be the ground level or a long-lived excited level. Depending on the experimental resolution and the natural widths of the intermediate excited levels, individual

resonances can be separated in the measured photoionization spectrum, i.e., in the cross section for the production of ions in a given charge state as a function of photon energy.

With sufficient experimental resolution, the natural width of each individual resonance can be determined. From the absolute measurement of the photoionization cross section σ the resonance strength, which is essentially the peak area under the resonance,

$$S = \int_{E_\gamma} \sigma(E_\gamma) dE_\gamma \tag{A1}$$

is obtained. E_γ is the photon energy. This definition of S follows the experiment-oriented approach pursued, for example, in the treatment by Thorne [33], who defines an integrated absorption coefficient k which is related to the absorption oscillator strength f_{ik} via

$$\int_\nu k(\nu) d\nu = \frac{e^2}{4\epsilon_0 m_e c} n_1 f_{ik}, \tag{A2}$$

where ν is the frequency of the absorbed light, e is the elementary charge, ϵ_0 is the electric constant, m_e is the electron rest mass, c is the vacuum speed of light, and n_1 is the number of absorbing atoms in state $|i\rangle$ per unit volume. A beam of photons passing the distance x through the absorbing dilute medium is attenuated by the factor $\exp(-kx) = \exp(-\sigma n_1 x)$. By replacing $k(\nu)$ in Eq. (A2) with σn_1 and multiplying both sides of the equation with Planck's constant h and dividing by n_1, one obtains

$$S = \int_{E_\gamma} \sigma(E_\gamma) dE_\gamma = \frac{he^2}{4\epsilon_0 m_e c} f_{ik} = 109.761 \ \text{Mb eV} f_{ik}. \tag{A3}$$

Since S follows from measured cross sections, it is possible to derive the absorption oscillator strength from the experiment.

Equation (A2) is valid under the assumption that quantum mechanical interferences between resonant and nonresonant as well as between neighboring resonances can be neglected. As in the present experiment, the intermediate core-excited level may undergo different Auger processes and cascades of Auger decays may be possible, leading to different final charge states of the initial atom or ion. Each channel is described by a cross section $\sigma_{\rm ne}$ with n characterizing the number of electrons removed from the initial atom or ion. The intermediate excited level can also decay by the emission of electromagnetic radiation. The associated channel has not been observed in merged-beam photon-ion experiments so far, yet it is possible to extract information on the rate for radiative transitions. As an example, photoexcitation of ground-term $C^+(1s^2 2s^2 2p\ ^2P)$ ions to K-shell-excited $C^+(1s 2s^2 2p^2\ ^2D)$ and $C^+(1s 2s^2 2p^2\ ^2P)$ is discussed below. Absolute cross sections σ_{1e}, σ_{2e}, and σ_{3e} for net single, double, and triple photoionization, respectively, are included in Fig. 1 and separately displayed in Fig. 6.

From a detailed high-resolution experiment, like the present one, the resonance energy $E_{\rm res}$ and the natural width Γ can be obtained as well as the resonance strength $S_{\rm ne}$ for each of the n-electron-removal channels

$$S_{\rm ne} = \int_{E_\gamma} \sigma_{\rm ne}(E_\gamma) dE_\gamma. \tag{A4}$$

The number n of electrons finally removed from the parent atom or ion depends on the atomic number, the charge state, the level structure and on the core-hole state populated in the photoabsorption process. For the present examples, at most $n = 3$ electrons were removed. The cross section for net triple photoionization is already very small (by a factor of $\approx 10^{-4}$ compared to single photoionization).

The transition wavelength λ_{ik} follows immediately as

$$\lambda_{ik} = hc/E_{\text{res}} = 1239.8419739 \text{ nm eV}/E_{\text{res}} \quad \text{(A5)}$$

(the 2014 CODATA values for fundamental physical constants provided by the $\underline{Co}$mmittee on $\underline{Data}$ of the International Council for Science are used throughout this paper). The lifetime τ of the intermediate resonant level is

$$\tau = \hbar/\Gamma = 6.582119514 \times 10^{-16} \text{ eV s}/\Gamma \quad \text{(A6)}$$

with $\hbar$, as usual, equal to Planck's constant divided by 2π.

Next, the absorption oscillator strength f_{ik} follows from the absorption resonance strength S. This quantity is the sum of the individual resonance strengths of all decay channels

$$S = S_{1e} + S_{2e} + S_{3e} + S_\gamma. \quad \text{(A7)}$$

So far, the resonance strength contained in the photon-emission channels is not known and photoemission is not observed. However, the absorption oscillator strength f_{ik} for the transition from the initial level $|i\rangle$ to the intermediate autoionizing level $|k\rangle$ is directly related to the Einstein coefficient A_{ki}, which describes the rate of radiative decay from level $|k\rangle$ to level $|i\rangle$. The oscillator strength follows from the relation [see Eq. (A3)]

$$f_{ik} = S \frac{4\epsilon_0 m_e c}{he^2} = S \times 9.1107 \times 10^{-3} \text{ (Mb eV)}^{-1}. \quad \text{(A8)}$$

The oscillator strength f_{ik} for an electric dipole transition $i \rightarrow k$ can also be expressed by its relation with the transition rate A_{ki} [35]

$$f_{ik} = 1.4992 \times 10^{-14} \text{ s/nm}^2 \times \lambda_{ki}^2 \frac{g_k}{g_i} A_{ki}, \quad \text{(A9)}$$

where g_k and g_i are the statistical weights of $|k\rangle$ and $|i\rangle$, respectively. The sum of all transition rates for radiative decays to final levels $|f\rangle$ provides the partial width Γ_γ of the resonant intermediate level

$$\Gamma_\gamma = \hbar \sum_f A_{kf}. \quad \text{(A10)}$$

For the present examples of K-shell resonance transitions in C^+, the only relevant radiative-decay paths of the intermediate $C^+(1s2s^2 2p^2 \, ^2D)$ and $C^+(1s2s^2 2p^2 \, ^2P)$ levels lead back to the $C^+(1s^2 2s^2 2p \, ^2P)$ initial term so that

$$\Gamma_\gamma = \hbar A_{ki}. \quad \text{(A11)}$$

With the equations given above and the expectation that radiative decay is much less probable than Auger decay, S and f_{ik} can be iteratively determined.

In the first approximation, one can set

$$S^{(1)} = S_{1e} + S_{2e} + S_{3e} \quad \text{(A12)}$$

and derive

$$f_{ik}^{(1)} = S^{(1)} \times 9.1107 \times 10^{-3} \text{ (Mb eV)}^{-1} \quad \text{(A13)}$$

and hence a first approximation of the radiative width of the intermediate excited state is given by

$$\Gamma_\gamma^{(1)} = \hbar A_{ki}^{(1)} = \hbar f_{ik}^{(1)} \frac{g_i}{g_k} / \left(1.4992 \times 10^{-14} \text{ s/nm}^2 \times \lambda_{ki}^2\right). \quad \text{(A14)}$$

In addition, a first approximation of the resonance strength for radiative decay of the intermediate excited state can be derived as

$$S_\gamma^{(1)} = S^{(1)} \frac{\Gamma_\gamma^{(1)}}{\Gamma}. \quad \text{(A15)}$$

For the examples under discussion, $S_\gamma^{(1)}$ is approximately 2×10^{-3} to 1.1×10^{-2} of $S^{(1)}$; i.e., the correction of $S^{(1)}$ is at least an order of magnitude smaller than the experimental uncertainty of $S^{(1)}$. It is therefore justified to set

$$S = S^{(2)} = S^{(1)} + S_\gamma^{(1)}. \quad \text{(A16)}$$

With S now known, f_{ik} follows from Eq. (A8) and then

$$A_{ki} = f_{ik} \frac{g_i}{g_k} / \left(1.4992 \times 10^{-14} \text{ s/nm}^2 \times \lambda_{ki}^2\right). \quad \text{(A17)}$$

The partial widths for n-electron removal are readily obtained from

$$\Gamma_{\text{ne}} = \frac{S_{\text{ne}}}{S} \Gamma \quad \text{(A18)}$$

and the Auger decay rates for the emission of n electrons are

$$A_{\text{ne}} = \Gamma_{\text{ne}}/\hbar. \quad \text{(A19)}$$

All these quantities have been derived from the measurement of $1s \rightarrow 2p$ excitations of C^+ and are listed in Table I. As far as available, they are compared with the literature in Table II.

[1] M. F. Hasoğlu, S. A. Abdel-Naby, T. W. Gorczyca, J. J. Drake, and B. M. McLaughlin, Astrophys. J. **724**, 1296 (2010).

[2] A. S. Schlachter, M. M. Sant'Anna, A. M. Covington, A. Aguilar, M. F. Gharaibeh, E. D. Emmons, S. W. J. Scully, R. A. Phaneuf, G. Hinojosa, I. Álvarez, C. Cisneros, A. Müller, and B. M. McLaughlin, J. Phys. B: At. Mol. Opt. Phys. **37**, L103 (2004).

[3] A. Müller, A. Borovik, Jr., T. Buhr, J. Hellhund, K. Holste, A. L. D. Kilcoyne, S. Klumpp, M. Martins, S. Ricz, J. Viefhaus, and S. Schippers, Phys. Rev. Lett. **114**, 013002 (2015).

[4] E. Jannitti, M. Gaye, M. Mazzoni, P. Nicolosi, and P. Villoresi, Phys. Rev. A **47**, 4033 (1993).

[5] H. Kjeldsen, F. Folkmann, H. Knudsen, M. S. Rasmusssen, J. B. West, and T. Andersen, Astrophys. J. **524**, L143 (1999).

[6] H. Kjeldsen, J. E. Hansen, F. Folkmann, H. Knudsen, J. B. West, and T. Andersen, Astrophys. J. Suppl. Ser. **135**, 285 (2001).

[7] G.-L. Wang and X.-X. Zhou, Chin. Phys. **16**, 2361 (2007).

[8] Y.-L. Shi and C.-Z. Dong, Acta Phys. Sin. **58**, 2350 (2009).

[9] M. F. Gharaibeh, N. El Hassan, M. M. Al Shorman, J. M. Bizau, D. Cubaynes, S. Guilbaud, I. Sakho, C. Blancard, and B. M. McLaughlin, J. Phys. B: At. Mol. Opt. Phys. **47**, 065201 (2014).

[10] B. M. McLaughlin, J. M. Bizau, D. Cubaynes, M. M. Al Shorman, S. Guilbaud, I. Sakho, C. Blancard, and M. F. Gharaibeh, J. Phys. B: At. Mol. Opt. Phys. **47**, 115201 (2014).

[11] J. K. Rudolph, S. Bernitt, S. W. Epp, R. Steinbrügge, C. Beilmann, G. V. Brown, S. Eberle, A. Graf, Z. Harman, N. Hell, M. Leutenegger, A. Müller, K. Schlage, H.-C. Wille, H. Yavaş, J. Ullrich, and J. R. C. López-Urrutia, Phys. Rev. Lett. **111**, 103002 (2013).

[12] R. Steinbrügge, S. Bernitt, S. W. Epp, J. K. Rudolph, C. Beilmann, H. Bekker, S. Eberle, A. Müller, O. O. Versolato, H.-C. Wille, H. Yavaş, J. Ullrich, and J. R. C. López-Urrutia, Phys. Rev. A **91**, 032502 (2015).

[13] A. Müller, Phys. Scr. **90**, 054004 (2015).

[14] J. M. Bizau, D. Cubaynes, S. Guilbaud, M. M. Al Shorman, M. F. Gharaibeh, I. Q. Ababneh, C. Blancard, and B. M. McLaughlin, Phys. Rev. A **92**, 023401 (2015).

[15] A. Müller, A. Borovik, Jr., T. Buhr, J. Hellhund, K. Holste, A. L. D. Kilcoyne, S. Klumpp, M. Martins, S. Ricz, J. Viefhaus, and S. Schippers, J. Phys. Conf. Ser. **635**, 012033 (2015).

[16] S. Schippers, R. Beerwerth, L. Abrok, S. Bari, T. Buhr, M. Martins, S. Ricz, J. Viefhaus, S. Fritzsche, and A. Müller, Phys. Rev. A **94**, 041401(R) (2016).

[17] A. Müller, D. Bernhardt, A. Borovik, Jr., T. Buhr, J. Hellhund, K. Holste, A. L. D. Kilcoyne, S. Klumpp, M. Martins, S. Ricz, J. Viefhaus, and S. Schippers, Astrophys. J. **836**, 166 (2017).

[18] S. Schippers, M. Martins, R. Beerwerth, S. Bari, K. Holste, K. Schubert, J. Viefhaus, D. W. Savin, S. Fritzsche, and A. Müller, Astrophys. J. **849**, 5 (2017).

[19] S. Schippers, S. Ricz, T. Buhr, A. Borovik, Jr., J. Hellhund, K. Holste, K. Huber, H.-J. Schäfer, D. Schury, S. Klumpp, K. Mertens, M. Martins, R. Flesch, G. Ulrich, E. Rühl, T. Jahnke, J. Lower, D. Metz, L. P. H. Schmidt, M. Schöffler, J. B. Williams, L. Glaser, F. Scholz, J. Seltmann, J. Viefhaus, A. Dorn, A. Wolf, J. Ullrich, and A. Müller, J. Phys. B: At. Mol. Opt. Phys. **47**, 115602 (2014).

[20] S. Schippers, A. Borovik, Jr., T. Buhr, J. Hellhund, K. Holste, A. L. D. Kilcoyne, S. Klumpp, M. Martins, A. Müller, S. Ricz, and S. Fritzsche, J. Phys. B: At. Mol. Opt. Phys. **48**, 144003 (2015).

[21] J. Viefhaus, F. Scholz, S. Deinert, L. Glaser, M. Ilchen, J. Seltmann, P. Walter, and F. Siewert, Nucl. Instrum. Methods **A710**, 151 (2013).

[22] R. A. Phaneuf, C. C. Havener, G. H. Dunn, and A. Müller, Rep. Prog. Phys. **62**, 1143 (1999).

[23] A. Müller, S. Schippers, R. A. Phaneuf, S. W. J. Scully, A. Aguilar, A. M. Covington, I. Álvarez, C. Cisneros, E. D. Emmons, M. F. Gharaibeh, G. Hinojosa, A. S. Schlachter, and B. M. McLaughlin, J. Phys. B: At. Mol. Opt. Phys. **42**, 235602 (2009).

[24] A. E. Kramida, Y. Ralchenko, J. Reader, and NIST ASD Team, NIST Atomic Spectra Database (ver. 5.3), http://physics.nist.gov/asd.

[25] Y. Sun, F. Chen, and B. C. Gou, J. Chem. Phys. **135**, 124309 (2011).

[26] R. D. Cowan, *The Theory of Atomic Structure and Spectra* (University of California Press, Berkeley, 1981).

[27] C. J. Fontes, H. L. Zhang, J. Abdallah, Jr., R. E. H. Clark, D. P. Kilcrease, J. Colgan, R. T. Cunningham, P. Hakel, N. H. Magee, and M. E. Sherrill, J. Phys. B: At. Mol. Opt. Phys. **48**, 144014 (2015).

[28] C.-Z. Dong (private communication).

[29] M. H. Chen and B. Crasemann, At. Data Nucl. Data Tables **38**, 381 (1988).

[30] M. F. Hasoğlu, T. W. Gorczyca, K. T. Korista, S. T. Manson, N. R. Badnell, and D. W. Savin, Astrophys. J. **649**, L149 (2006).

[31] P. Liu, J. Zeng, and J. Yuan, arXiv:1709.08796 [physics.atom-ph].

[32] F. Zhou, Y. Ma, and Y. Qu, Phys. Rev. A **93**, 060501(R) (2016).

[33] A. P. Thorne, *Spectrophysics*, 2nd ed. (Chapman and Hall, London, 1988).

[34] W. C. Martin and W. L. Wiese, in *Springer Handbook of Atomic, Molecular, and Optical Physics*, edited by G. W. F. Drake (Springer, New York, 2006), Chap. 10, pp. 175–198.

[35] W. L. Wiese and J. R. Fuhr, J. Phys. Chem. Ref. Data **38**, 565 (2009).